SHOCK-WAVE AND HIGH-STRAIN-RATE PHENOMENA IN MATERIALS

EDITED BY

MARC A. MEYERS

University of California, San Diego
La Jolla, California

LAWRENCE E. MURR

University of Texas at El Paso
El Paso, Texas

KARL P. STAUDHAMMER

Los Alamos National Laboratory
Los Alamos, New Mexico

Marcel Dekker, Inc. New York • Basel • Hong Kong

48

High Strain, High-Strain-Rate Deformation of Copper

M. A. MEYERS, L. W. MEYER**,J. BEATTY*, U. ANDRADE, K. S. VECCHIO, and A. H. CHOKSHI

University of California, San Diego
La Jolla, California 92093, U.S.A.

*U.S. Army Materials Technology Laboratory, Watertown, Massachusetts, U.S.A.

**IFAM, Bremen, West Germany

While copper exhibits total elongations that typically do not exceed 0.5 at low strain rates, the strains exceed 10 in tension under the special conditions imposed during shaped-charge deformation. The reasons for this extended plasticity are poorly understood and the role of microstructural evolution has not been examined in any detail. Residual microstructures produced in shaped charges (jets and slugs) and in special Hopkinson bar tests in which high strains and strain rates were imposed are characterized by optical and transmission electron microscopy. The microstructure was preconditioned by shock loading it to a pressure of 40 GPa in order to enhance heat generation during subsequent high-strain-rate plastic deformation. This preconditioning simulates shock-wave strengthening of the shaped charge liner prior to its collapse. The residual structures can exhibit recrystallized regions. By means of heat transfer calculations, it is shown that the cooling in the shaped charges slugs and jets takes place over seconds, while in the especially designed experiments it takes place over milliseconds. Therefore, the microstructures investigated under the special testing configurations are closer to the ones existing during deformation.

The basic equations that govern dynamic recrystallization as they apply to high-strain rate deformation are presented, and the plastic response of the copper after having undergone these microstructural changes is discussed.

I. OBSERVATIONS ON SHAPED CHARGES

The enhanced ductility exhibited in uniaxial and biaxial tension by metals under dynamic deformation is of great importance. Examples are the large extensions undergone by shaped charge jets and the extensive plastic deformations undergone by space shields when subjected to hypervelocity impact, forming a plume. A number of investigations have treated the problem of an extending jet analytically; Chou and Carleone [1], Walsh [2], and Grady [3] performed stability analyses on stretching plastic jets. The effect of lateral inertia was incorporated by Grady [3], Fressengeas and Molinari [4], and Romero [5], based on observations by Walsh [2] and Frankel and Weihs [6]. It was found that a confining pressure is produced by the gradient in radial velocities resulting from the rapid longitudinal stretching. This inertial confining pressure has the effect of inhibiting failure by internal void formation. Grady [3] estimated that this pressure could be as high as 10 Y at a strain rate of 10^5 s^{-1}, where Y is the yield stress. These studies have successfully predicted times-to-failure and fragment sizes. However, there still remain many unknown aspects in shaped-charge deformation, and microstructural evolution in both liner collapse and jet stretching is virtually unknown. Jamet [7,8] performed flash X-ray diffraction experiments on aluminum jets using transmitted X-rays, and on copper jets using reflected X-rays. For aluminum, he conclusively showed that the jet was solid. For copper jets, the reflected mode could only identify the surface which was shown to be crystalline (i.e. solid).

In this report these microstructural evolution processes will be addressed. First, observations made on slug and jet fragments are described. Second, special experiments in which high strains are applied at a high strain rate are presented. And third, dynamic recrystallization at high strain rates is described analytically by two models, which are developed in detail elsewhere [9, 10].

The recovery of jets and slugs is not simple. Jets propelled at velocities approaching 10^4 ms^{-1} have to be decelerated without subsequent damage. Two slugs were obtained, from D. A. Lassila (Lawrence Livermore National Laboratory) and from C. Wittman (Honeywell). Figure 1 shows micrographs from these two slugs taken from longitudinal and transverse sections. The microstructures exhibit, typically, a recrystallized

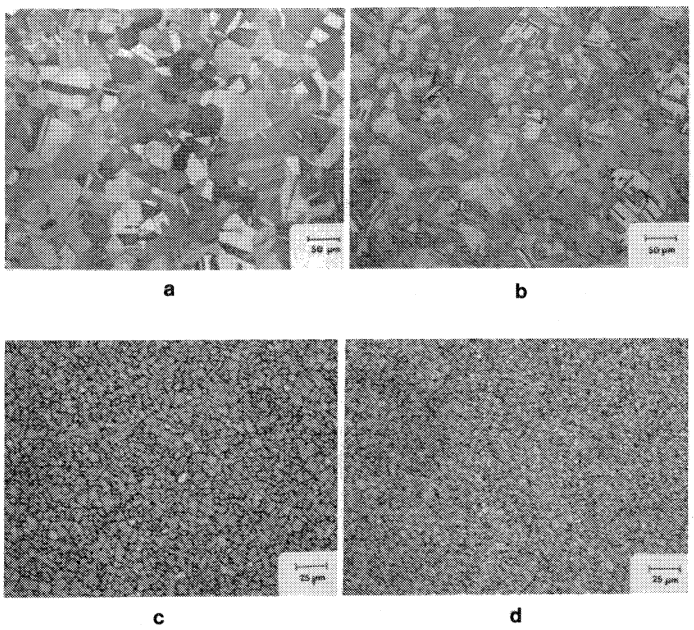

FIG. 1 *Typical optical micrographs from Lassila (a,b) and Wittman (c,d) slugs; (a and c) transverse sections: (b and d) longitudinal sections.*

morphology. The absence of grain elongation, in the longitudinal section, in spite of the large strains undergone by the slug, shows that recrystallization occurred. Nevertheless, there is a significant difference in grain size between the two materials: it is equal to 40 μm for the Wittman slug, while it appears to be less than 5 μm for the Lassila slug. A small jet section was also characterized and it is shown in Fig. 2. The optical micrograph shows a recrystallized structure (grains equiaxed), as evidenced in Fig. 2(a), with a grain size of ~30 μm. Transmission electron microscopy of this jet fragment shows some evidence of dislocation activity, 2b, and deformation twins, 2c; most of the regions were, however, simply recrystallized.

On the other hand, preliminary transmission electron microscopy of the slug provided by Lassila showed a microcrystalline structure with low dislocation density [9]. Other investigators (Jamet [11]; Hirsch [12]; Buchar [13]) observed columnar grains surrounding voids in slugs. This is strongly suggestive of melting pockets forming within the slug. Upon solidification, shrinkage produces the void; the solidification grains are elongated, and their longitudinal axes converge towards the center of the void. The

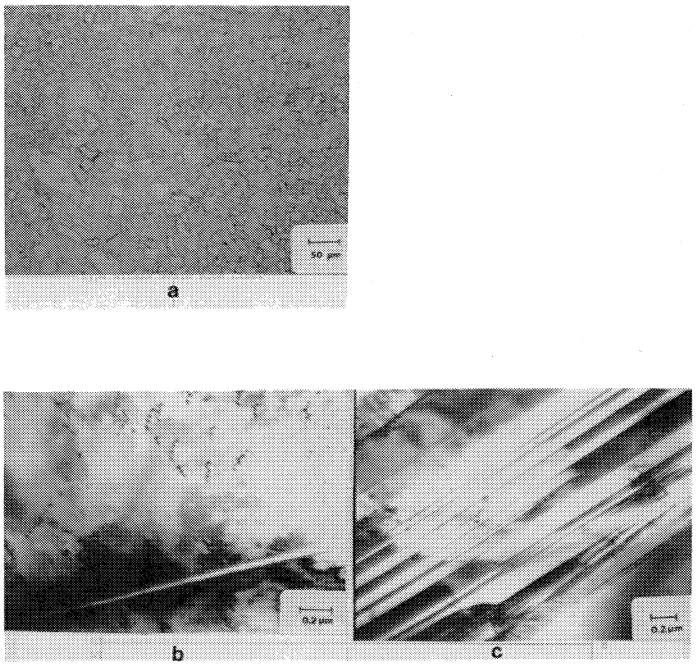

FIG. 2 *Jet section: (a) optical micrograph; (b) and (c) transmission electron micrographs.*

conclusions that can be drawn from the above observations are: (a) considerable variation in microstructure exists; (b) recrystallization (static) can destroy a great extent of the deformation structure; and (c) some melt pockets probably exist, but the jet is at least partially solid.

The temperature rises experienced by the slug and jet are a direct consequence of the adiabaticity of the plastic deformation process. The adiabatic temperature rise in copper can be calculated based on the plastic deformation energy. It is known that ~90% of deformation energy is converted to heat. The temperature rise, ΔT is

$$\Delta T = \frac{0.9}{\rho c_p} \int_0^{\varepsilon} \sigma \, d\varepsilon \tag{1}$$

where ε is the plastic strain, σ is the flow stress, ρ is the density of the material, and c_p is the heat capacity.

The following simple constitutive model for the stress as a function of homologous temperature, T_h (=T/T_m, where T is absolute temperature and T_m is the absolute melting temperature), strain, and strain rate was proposed by Johnson and Cook [14]:

$$\sigma = (\sigma_0 + B\varepsilon^N)(1 + C\ell n\dot{\varepsilon}^*)(1 - T_h^M) \tag{2}$$

where σ_0 is the yield stress, B, C, N, and M are constants and $\dot{\varepsilon}^*$ ($= \dot{\varepsilon}/\dot{\varepsilon}_0$) is the normalized strain rate ($\dot{\varepsilon}$ is the imposed strain rate and $\dot{\varepsilon}_0 = 1\ s^{-1}$). Equations 1 and 2 may be combined as follows by assuming a constant strain rate:

$$\int_{T_0^*}^{T_f^*} \frac{dT}{1 - T_h^M} = \frac{0.9\,(1 + C \ln \dot{\varepsilon}^*)}{c_p\,\rho} \int_0^{\varepsilon_f} (\sigma_0 + B\varepsilon^N)\, d\varepsilon \tag{3}$$

where T_0^* and T_f^* are the initial and final homologous temperature, respectively. The solution to Eqn. 3 gives the temperatures rise as a function of plastic deformation.

Calculations for a typical Cu shaped charge reveal that the strain rates achieved are of the order of $>10^4\ s^{-1}$. Johnson and Cook [14] reported a value of M = 1.09 for Cu; for the purposes of the present approximate calculations, it is assumed that M = 1 in Eqn. 3. The temperature rise occurring during the dynamic deformation of Cu at room temperature and at a strain rate of $10^4\ s^{-1}$ was estimated using values of the other parameters reported by Johnson and Cook [14].

An analysis based on Equation 3 reveals that temperatures of >0.4 T_m may be achieved by plastic strains of ≈ 3 [9]. It is also noted that an increase in the yield stress, by shock hardening, decreases the strain necessary to achieve a given temperature. Recrystallization generally occurs at temperatures of >0.4 T_m. Approximate calculations show that shaped charges experience strains of ≈5 during the initial collapse. Consequently, the compressive deformation of shaped charges satisfies the experimental conditions necessary for recrystallization.

Jamet [11] measured the temperature attained in copper jets produced from 81.3 mm cones. He found values ranging from 428 to 537° C (0.5 to 0.6 T_m). These values are consistent with the above calculations and well within the realm of recrystallization.

II. CONTROLLED RECOVERY EXPERIMENTS

The temperature history of slugs and jets determines the residual microstructures. The total deformation occurs in approximately 0.3 ms. This is computed approximately by

$$t = t_D + t_t \tag{4}$$

where t_D is the time taken for the detonation front to propagate through the charge and t_t is the travel time of the jet. These values are obviously dependent on geometry, and a cone with apex height of 10 cm was used; the travel distance of the jet was assumed to be 20 cm. The total cooling of the jet and slug are dependent on their initial temperature, mass, shape, and cooling medium. Carslaw and Jaeger [15] provide a formalism for the calculations of heat transfer from a perfect cylindrical conductor into a surrounding medium. Assuming that the slug and jet are cooled in sand, a common decelerating medium for shaped charges, one can estimate the cooling rate for the center along the axis of cylinders with 1 cm (simulating slug) and 1 mm (simulating jet) diameters. Figure 3(a)

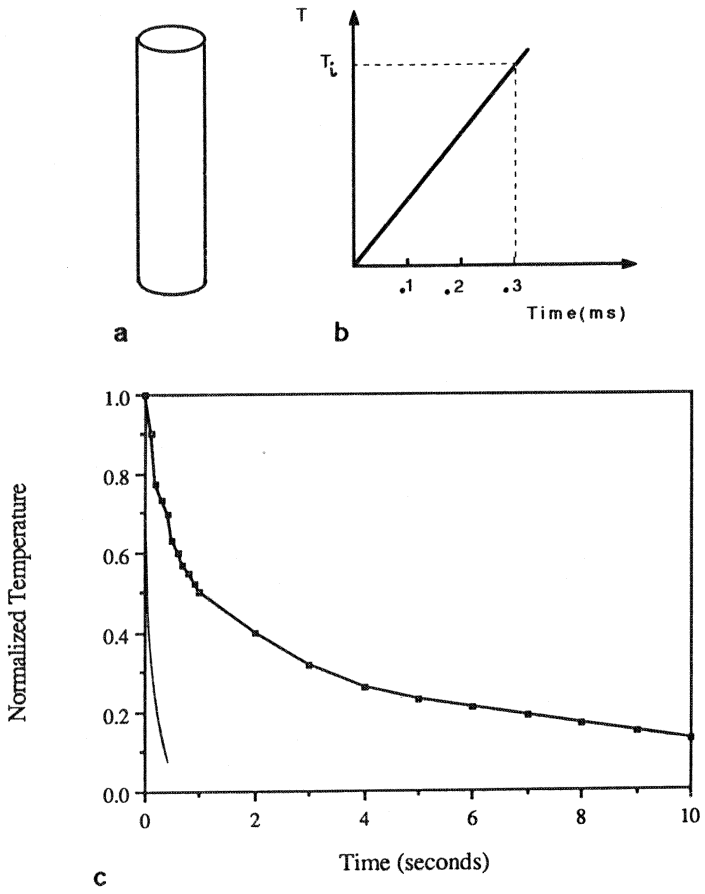

FIG. 3(a) *Geometry used for calculating cooling of slug and jet; (b) heating as a function of time (deformation); (c) cooling in sand; of slug (1 cm diameter) and jet (1 mm diameter).*

shows the idealized geometry (infinitely long cylinder), while Fig. 3(b) schematically shows a linear heating within 0.3 ms. By using appropriate heat capacities and thermal diffusivities, one obtains the curves displayed in Fig. 3(c). The normalized temperature, equal to the ratio: $(T - T_0)/(T_i - T_0)$ is plotted as a function of time after deformation stops. T is the current temperature, T_i the initial temperature of the slug (or jet) and T_0 the surrounding temperature. It can be seen that the cooling takes place over a number of seconds for the slug and over a fraction of a second for a jet. This order of magnitude calculation indicates that thermal recovery processes are most likely to alter the deformation substructure developed during deformation if the temperature reaches a level of 0.4-0.5 T_m. The discussion in Section I shows that this is the case. The exposure to temperature during cooling is approximately one thousand times longer than during deformation (.3ms). For this reason, it is felt that special recovery experiments need to be devised to:

(a) produce high-strain, high-strain-rate deformation with real-time diagnostics, under controlled conditions,

(b) provide rapid cooling after deformation to reduce, as much as possible, post-deformation structural recovery processes (recovery, recrystallization, and grain growth.)

Two experimental geometries were tested as described below. They utilize the Hopkinson bar and well-controlled, well-characterized stress pulses. The two geometries are shown in Fig. 4. The disk-shaped specimens have been used directly between the striker and the incident bars; they can also be placed between the incident and transmitter bars. The reductions in thickness accomplished were as high as 80 pct.,which corresponds to a true strain of 1.6. By comparison, a tensile elongation of 400% is necessary to obtain a true strain of 1.6. Copper disks with an initial thickness of 0.5 mm were impacted at ~ 100 m/s; the resulting microstructures are shown in Fig. 5. Different areas exhibited different structures; while a large proportion of the deformed material exhibited a high density of dislocations (Fig. 5(a)), there were some recrystallized areas present (Fig. 5(b)). The grain boundaries are irregular, indicating a high mobility. Figure 5(c) shows a small recrystallized region within which one can see some dislocations. The presence of dislocations inside recrystallized regions is usually considered evidence for dynamic recrystallization. However, in the present case the results are too preliminary to allow a positive identification.

The hat-shaped configuration, developed by Hartman, Kunze, and Meyer [16], and shown in Fig. 4(b), provides shear concentration in the regions circled. The stress pulse, produced by impacting the incident bar, generates controlled plastic shear deformation in the regions indicated, while the specimen itself undergoes mostly elastic deformation. The spacer ring establishes the limit for the plastic deformation within the shear zone. The gap between the incident bar and the ring is exaggerated in Fig. 4(b). A typical longitudinal

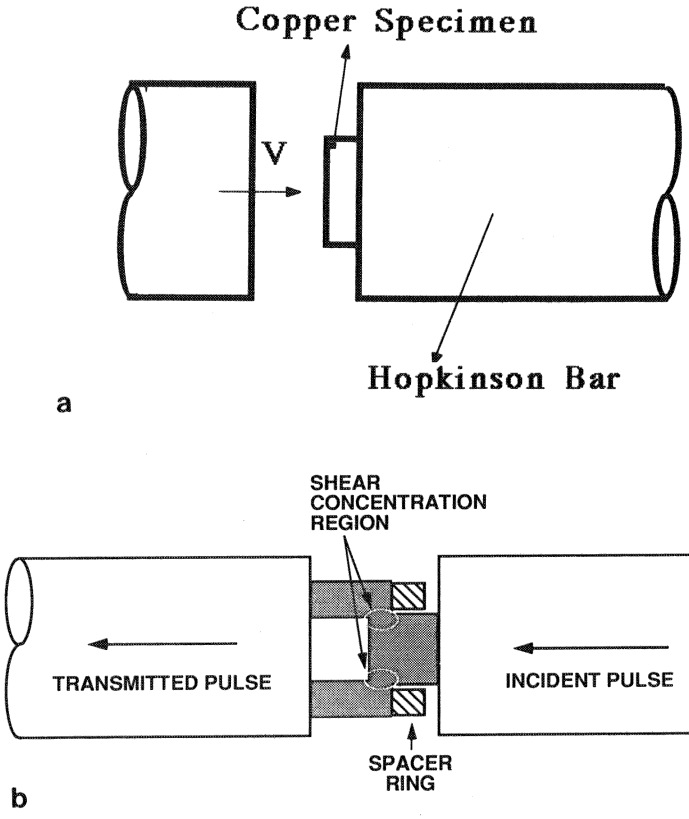

FIG. 4 *Experimental geometries for controlled high strain, high strain-rate experiments; (a) disc-shaped specimen; (b) hat-shaped specimen.*

section of specimen after impact is shown in Fig. 6(a). Copper was tested in the Hopkinson bar under two different conditions : 1) annealed, and 2) shock-hardened to a pressure of ~40 GPa by impact with a copper plate. The shock hardening procedure is described in detail in, e.g., DeCarli and Meyers [17]. An explosive lens initiated a 2.54-cm thick slab of PBX 9404 explosive, which accelerated a 4.7 mm thick stainless steel plate, impacting a properly momentum-trapped copper block. Velocity pins were used to determine the impact velocity. The average of three readings was 2,200 m/s. Shock hardening of the copper simulates the microstructural hardening process undergone by a shaped charge when the explosive detonates in contact with it.

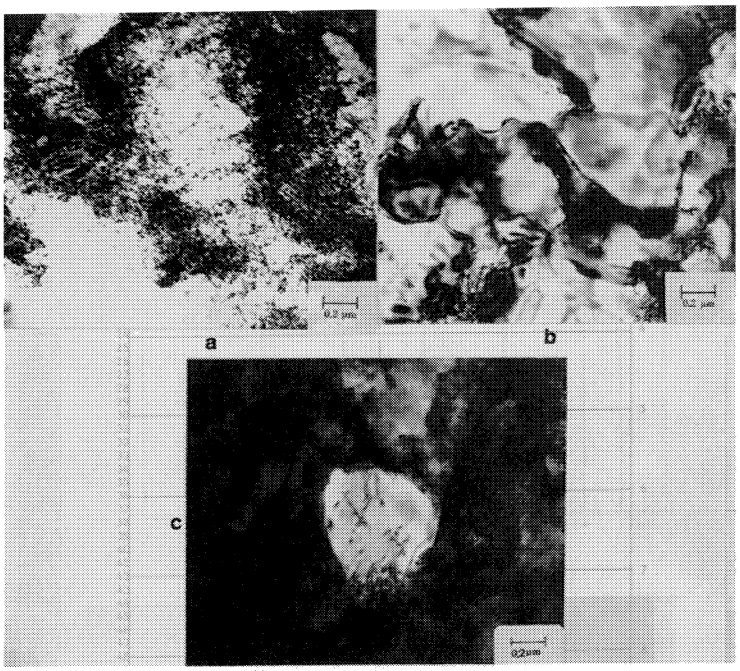

FIG. 5 *Copper disk specimens impacted in Hopkinson bar (ε_{eng} ~1.7); (a) dislocated region; (b) fully recrystallized region; (c) partially recrystallized region.*

Optical micrographs of the shear concentration regions for both annealed and pre-shocked specimens are shown in Fig. 6(b) and 6(c). There are significant differences between the two shear localization regions. The width of the band is larger for the annealed (~400 μm) than for the pre-shocked (~200 μm) specimen. This increased localization of the shocked specimen is the direct result of a decreased work hardening during deformation and is a well-known characteristic of the material. Within the band in the pre-shocked specimen, most microstructural features are annihilated. The microstructure of the shocked material exhibits a large incidence of deformation twins, which are known to be produced by shock loading. Within the band in the pre-shocked material (which had undergone a localized shear strain of 0.8 at a strain rate of ~ $10^5 s^{-1}$), the individual grain boundaries are not visible any longer under optical observation. Transmission electron microscopy was performed and the preliminary results are described herein. Figure 7 shows one of the features identified within the high strain region. Both

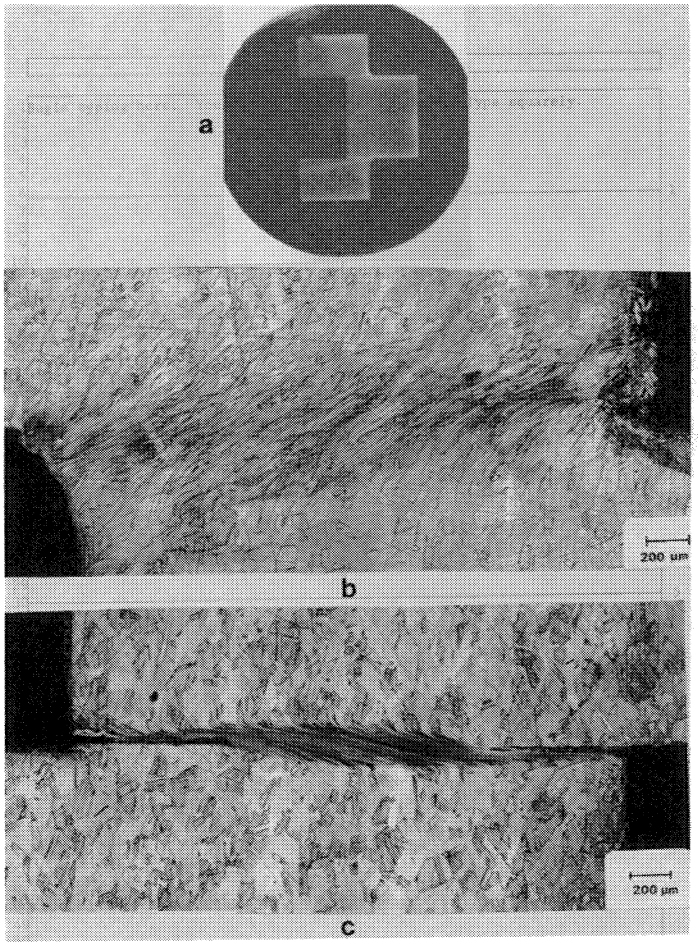

FIG. 6 *(a) Longitudinal section of copper hat specimen after impact; (b) and (c) shear concentration regions for annealed and shock-hardened specimens, respectively.*

the bright- and dark-field electron micrographs and the diffraction pattern give evidence of a fine microstructure. The sizes of the micrograins, as shown in the dark-field image, are approximately 0.05 µm. This microcrystalline structure is similar to the one observed for the copper shaped charge slug [9]. The cooling rates for the disk- and hat-shaped specimens, after high-strain rate deformation, are much higher than the ones encountered in shaped charges, and therefore the deformation structure is better retained. Preliminary heat transfer calculations can be conducted assuming a semi-infinite body. The thicknesses are assumed to be equal to the disk thickness and the shear localization width. Figure 8 shows

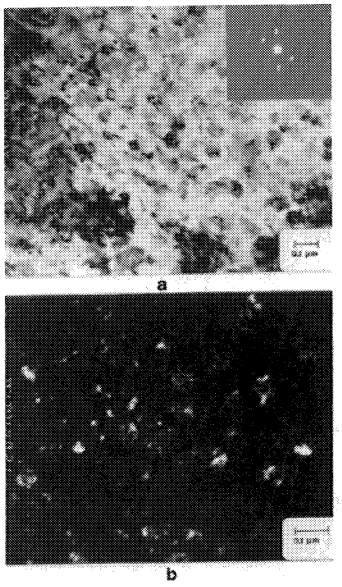

FIG. 7
Transmission electron micrograph of shear localization region $(\gamma = 8;\ \dot{\gamma} \cong 10^5\ sec^{-1})$ *in pre-shocked copper hat-shaped specimen; (a) bright field; (b) dark field.*

the post-deformation temperature histories for the two cases. The temperature distribution at time t = 0 is assumed to be a step function; the temperature is equal to T_0 in the surrounding material and equal to T_i within the band. The band has a thickness of 200 μm for both the disk- and the hat-shaped specimens (see Fig. 6a). The solution to the problem is provided by an error function (Carslaw and Jaeger [15]). Because of the higher diffusivity of copper (10x) than that of steel, the cooling rate is greater in the hat-shaped specimen. In contrast with the cooling undergone by a slug or jet in a normal recovery experiment, the cooling rate is on the order of one thousand times higher in the controlled recovery experiments described here. The cooling time is of the same order of magnitude as the deformation time (0.3 ms).

III. ANALYSIS OF PLASTIC DEFORMATION

The high strain rates, large strains, and large adiabatic temperature rises experienced by the material create a unique thermomechanical environment. It is premature to develop quantitative predictive analyses; nevertheless, based on the observations, some general principles can be outlined. The existing constitutive models for plastic deformation are based on dislocation motion. This dislocation motion is controlled by overcoming obstacles, viscous drag, or relativistic effects, as the imposed strain rate is increased. The model developed by Follansbee and Kocks [18,19] represents the most advanced formulation of these concepts. It also incorporates dislocation recovery as a softening

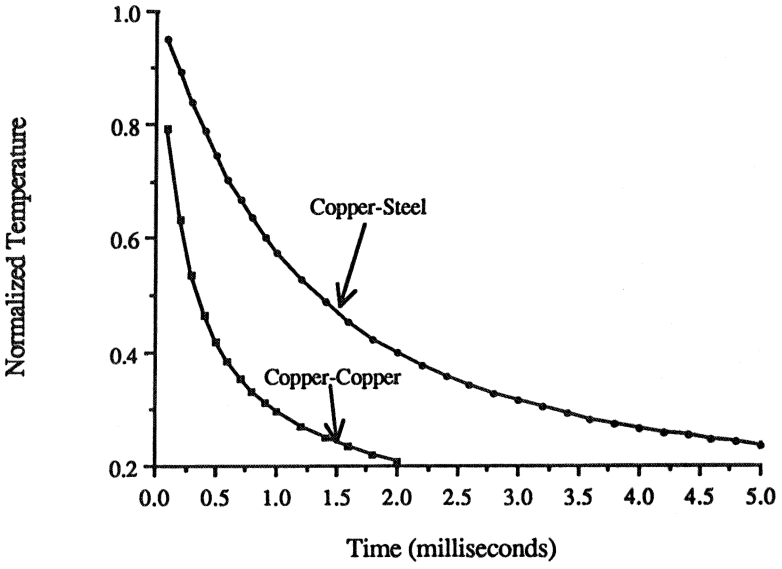

FIG. 8 *Computed normalized temperature* $(T_i - T) / (T_i - T_0)$ *for slab of 200 μm thickness surrounded by (1) copper (simulating hat-shaped specimen) and (2) steel (stimulating discoid specimen).*

process. These constitutive models are restricted to relatively low strains and we believe that the large imposed strains (in shaped charges, shear bands, and other hypervelocity events) require the incorporation of additional microstructural evolution mechanisms. We further propose that dynamic recrystallization plays a key role in this regime.

Dynamic recrystallization plays an important role in many plastic deformation processes. The experimental results and theoretical aspects of this phenomenon have been reviewed by McQueen and Baudelet [20], Sakai and Jonas [21], and Ueki et al. [22]. Dynamic recrystallization essentially involves the development of a dislocation cell and sub-grain structure and the transformation of low angle grain boundaries to high angle grain boundaries during plastic deformation. The process is repeated continuously during deformation, and leads eventually to the development of a steady-state recrystallized grain size, d_s. Dynamic recrystallization is a thermally activated process, which is important at temperatures greater than 0.4 T_m. From the theory for dynamic recrystallization developed by Sandstrom and Lagneborg [23] it is possible to obtain the recrystallized steady-state grain size. It is important to note that, in spite of the different approaches used by

Sandstrom and Lagneborg [23] and Derby and Ashby [24], both models predict the proportionality between the recrystallized grain size and $\dot{\varepsilon}^{0.5}$, where $\dot{\varepsilon}$ is the strain rate. Thus, at high strain rates one should expect small recrystallized grain sizes.

The mechanical response of this recrystallizing microstructure is not well understood yet. It is proposed that the inhibition of tensile instability in shaped charges is a direct consequence of this microstructural evolution. Both hypotheses lead to responses that are stable in tension. The first hypothesis is that classical superplasticity sets in; this occurs by grain boundary sliding. This is explained in detail by Chokshi and Meyers [9]. The second hypothesis is that dynamic recrystallization *per se* can lead to the desired response mechanism; a detailed account will appear shortly [10].

ACKNOWLEDGMENTS

This research was supported by the U. S. Army Research Office through Contracts DAAL03-88-K-0194, DAAL03-89-17-0396, and DAAL03-86-K0169. The use of the facilities of the Center of Excellence for Advanced Materials and of the Electron Optics and Microanalysis Facility at UCSD is gratefully acknowledged. Mr. U. Andrade was supported by the National Research Council (CNP), Brazil. The help of Mr. Jon Isaacs in carrying out the dynamic deformation experiments is gratefully acknowledged. Mr. Wittman (Honeywell) and Dr. D. Lassila (Lawrence Livermore National Lab) generously provided shaped charge specimens.

REFERENCES

1. P. C. Chou and J. Carleone, *J. Appl. Phys.*, 48: 4187 (1977).
2. J. M. Walsh, *J. Appl. Phys.*, 56: 1997 (1984).
3. D. E. Grady, *J. Impact Eng.*, 5: 285 (1987).
4. C. Fressengeas and A. Molinari, *Proc. Int. Conf. Mech. Prop. Materials at High Rates of Strain*, Inst. Phys. Conf. Ser. No. 102, p. 57, (1989).
5. L. A. Romero, *J. Appl. Phys.*. 65: 3006 (1989).
6. I. Frankel and D. Weihs, *J. Fluid Mech.*, 155: 289 (1985).
7. F. Jamet, "La Diffraction Instantanée," Report CO 227/84, Institut St. Louis, France, August 1984.
8. F. Jamet and R. Charon, "A Flash X-Ray Diffraction System for Shaped Charge Jets Analysis," Report CO 211/86, Institut St. Louis, France, June 1986.
9. A. H. Chokshi and M. A. Meyers, *Scripta Met.*, 24: 605 (1990).

10. M. A. Meyers, K. S. Vecchio, U. Andrade and A. H. Chokshi, unpublished results (1991).

11. F. Jamet, "Methoden zur Untersuchung der Physikalischen Eigenschaften eines Hohlladungstrahles," Report CO 227/82, Institut St. Louis, France, December 1982.

12. E. Hirsch, *Propellants and Explosives*, 6: 11 (1981).

13. J. Buchar, Institute of Physical Metallurgy, Czechoslovakia, private communication, 1990.

14. G. R. Johnson and W. H. Cook, *Proc. 7th Intern Symp. Ballistics*, Netherlands, 1983.

15. H. S. Carslaw and J. C. Jaeger, *Conduction of Heat in Solids*, Oxford, 2nd ed., 1959, pp. 55, 343.

16. K.-H. Hartman, H.-D. Kunze, and L. W. Meyer, in *Shock Waves and High-Strain Rate Phenomena in Metals*, eds. M. A. Meyers, and L. E. Murr, Plenum, N.Y. 1981, p. 325.

17. P. S. DeCarli and M. A. Meyers, in *Shock Waves and High-Strain Rate Phenomena in Metals*, eds. M. A. Meyers, and L. E. Murr, Plenum, N.Y. 1981, p. 341.

18. P. S. Follansbee, in *Metallurgical Applications at Shock-Wave and High Strain Rate Phenomena*, L. E. Murr, K. P. Staudhammer, and L. E. Murr eds., M. Dekker, 1986, p. 451.

20. H. J. McQueen and B. Baudelet, *Proc. ICSMA 5*, P. Haasen, V. Gerold and G. Kostorz, eds., Pergamon Press, Oxford, 1979, p. 329.

21. T. Sakai and J. J. Jonas, *Acta Met.*, 32: 189 (1984).

22. M. Ueki , S. Horie, and T. Nakamura, *Mater. Sci. Tech.* 3: 329, (1987).

23. R. Sandstrom and R. Lagneborg, *Acta. Met.*, 23: 387 (1975).

24. B. Derby and M. F. Ashby, *Scripta Met.*, 21: 879 (1987).